Ground and excited states of oxyheme: SAC/SAC-CI study

H. Nakatsuji [a,b,*], J. Hasegawa [a], H. Ueda [a], M. Hada [a]

[a] *Department of Synthetic Chemistry and Biological Chemistry, Faculty of Engineering, Kyoto University, Sakyo-ku, Kyoto 606-01, Japan*
[b] *Institute for Fundamental Chemistry, 34-4 Takano Nishi-Hiraki-cho, Sakyo-ku, Kyoto 606, Japan*

Received 19 November 1995; in final form 23 December 1995

Abstract

The SAC(symmetrie adapted cluster)/SAC-CI(configuration interaction) mehtod is applied to the ground and low-lying excited states of oxyheme ($FeC_{23}N_6O_2H_{16}$). The ground state ($^1A'$) is suitably represented by the Pauling model, Fe(II) ($S = 0$) + $O_2(^1\Delta_g)$. The SAC-CI result reproduces well the lower excitation spectrum of oxyhemoglobin. The lowest peak observed at 1.34 eV is assigned to the $^1\Delta_g \rightarrow {}^1\Sigma_g^+$ excitation of the O_2 ligand. Many transitions originating from the iron d orbitals are calculated, although their intensities are very small. The lowest triplet state ($1\,^3A''$), which is due to the $^1\Delta_g \rightarrow {}^3\Sigma_g^-$ transition around the O_2 ligand, is calculated at 0.47 eV above the ground state, but its level is sensitive to the electron correlations included. In the geometry of the deoxy form, this $1\,^3A''$ state becomes more stable than the closed-shell singlet state ($^1A'$), indicating a geometrical control of oxygen affinity of heme.

1. Introduction

Hemoglobin and myoglobin play an important role in mammalian life through the transport and storage of oxygen. Fe–porphyrin complex, called heme, constitutes their reaction center and binds oxygen reversibly [1]. Oxyheme which has oxygen O_2 at the sixth site and imidazole at the fifth site as a residue of histidine in protein is diamagnetic [2], while deoxyheme is in a high-spin state [3].

The nature of the Fe–O_2 bond in oxyheme has been studied both experimentally and theoretically and some review articles were published [1,3,4]. X-ray crystal structure analysis revealed an end-on oxygen binding structure [5]. Several models were proposed for the ground-state electronic structure of oxyheme. The Fe(II) ($S = 0$)–O_2 ($S = 0$) valence bond (VB) model by Pauling [6] is σ-donation from singlet oxygen ($^1\Delta_g$) and π back donation from the Fe d orbital. The Fe(II) ($S = 1$)–O_2 ($S = 1$) VB model by Goddard et al. and others [7,8] is based on the spin coupling between the two unpaired electrons on oxygen and on Fe(II). The Fe(III)–O_2^- model by Weiss [9] involves one-electron transfer from Fe to O_2, so that O_2 is regarded as superoxide.

Electron correlations are important for the description of the ground state of oxyheme [10,11]. Previous CI [12] and CASSCF [10] calculations gave different electronic structures for the ground states. For the triplet state, the previous CI calculation [12] failed to reproduce the energy ordering between the singlet ground state and the lowest triplet state. This indicates that a more elaborate study is necessary for the lower states of oxyheme.
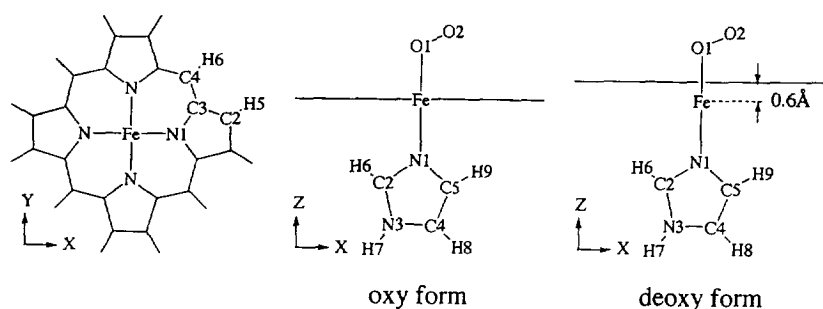
* Corresponding author.

Fig. 1. Geometries of oxyheme in the oxy and deoxy forms. The numbering of the atoms corresponds to those shown in Table 1.

The SAC (symmetry adapted cluster) [13]/SAC-CI (configuration interaction) [14] method [15] is suitable for calculating electron correlations in the ground and excited states of even relatively large systems like oxyheme. The theory is designed to be efficient and accurate and the calculational algorithms are rather flexible and not so restrictive to the computing system [15]. This method has successfully reproduced the electronic spectra of a wide variety of molecules [15], from water, formaldehyde, and ethylene to benzene, pyridine, metal complexes, and catalytic systems, and up to free base porphin (FBP) [16]. Note that the EOM-CC method by Bartlett et al. [17] belong to the SAC-CI method [18] published more than a decade ago than theirs. The differences they claimed [17] are quite a minor variation of the calculational method of the SAC-CI theory, which is formally exact. In this study, the ground and some low-lying singlet and triplet excited states of oxy-

heme are calculated by the SAC/SAC-CI method and the electronic structures and the spectrum of these states are discussed.

2. Computational details

The geometry of oxyheme is taken from the X-ray crystallographic data [19] for oxyhemoglobin of sperm whale with some small modifications. The porphyrin skeleton is fixed to D_{4h} symmetry and the entire molecular symmetry to C_s symmetry. The imidazole plane, one of the N_{Por}–Fe–N_{Por} axes, and the O–O axis are put on the mirror plane as shown in Fig. 1. The C–H distances in the porphyrin ring and in imidazole are taken from Refs. [20,21], respectively. The atomic coordinates are shown in Table 1.

Natural deoxyheme has a five-coordinated geome-

Table 1
Atomic coordinates of oxyheme (Å)

Segment	Atom [a]	x	y	z	Segment	Atom [a]	x	y	z
porphin	N1	1.9537	0.0	0.0	imidazole	N1	0.0	0.0	−2.0654
	C2	4.1889	0.6915	0.0		C2	−1.2095	0.0	−2.7916
	C3	2.8060	1.1297	0.0		N3	−0.8706	0.0	−4.2036
	C4	2.4702	2.4702	0.0		C4	0.5376	0.0	−4.2391
	H5	5.0604	1.3294	0.0		C5	1.0562	0.0	−2.9478
	H6	3.2339	3.2339	0.0		H6	−2.2826	0.0	−2.6693
oxygen [b]	O1	0.0	0.0	1.8267		H7	−1.5281	0.0	−5.0604
	O2	1.0979	0.0	2.3507		H8	1.0035	0.0	−5.2134
iron	Fe	0.0	0.0	0.0		H9	2.0637	0.0	−2.5587

[a] The numberings of the atoms in each segments are given Fig. 1.
[b] The lengths of Fe–O1, O1–O2, Fe–N_{Por}, and Fe–N_{Im} are 1.83, 1.21, 1.95, and 2.07 Å, respectively. The Fe–O1–O2 angle is 115.5°.

try in which Fe sits out of the porphyrin plane by 0.6 Å [22]. We also carry out the calculation of oxyheme in the geometry of the deoxy form, in which the porphyrin ring is moved towards oxygen by 0.6 Å along the $O–Fe–N_{Im}$ axis and all others are fixed at the oxyheme geometry.

The basis set for the porphyrin ring is of 2p double zeta quality, which is the same as our previous calculations for FBP [16]. For the Fe atom, we use Huzinaga's $(5333/53/5)/[53321/53/41]$ set [23] plus p-type polarization function ($\alpha = 0.082$) and for oxygen $(63/5)/[63/41]$ set [23] plus p-type anion basis ($\alpha = 0.059$) [23]. The basis set for imidazole is minimal; for C and N, $(63/5)/[63/5]$ set [23] and for H, $(4)/[4]$ set [24].

Hartree–Fock (HF) molecular orbitals (MOs) are used as the reference orbitals in the SAC/SAC-CI calculations. For the active space, higher 47 occupied MOs and lower 109 unoccupied MOs are used, and all the single excitations and the selected double excitations within this active space constitute the linked operators and their products the unlinked operators. The perturbative configuration selection procedure [16,25] is carried out for the main reference configurations, with the energy threshold 1×10^{-5} au for the ground state and 1×10^{-6} and 2×10^{-6} au for the singlet and triplet excited states, respectively. The resultant dimensions for the SAC/SAC-CI calculations are shown in Table 2. The program

HONDO [26] and the accelerated version [27] of the SAC85 [28] program are used for the HF and SAC/SAC-CI calculations.

3. Ground state electronic structure

First we analyze the HF orbitals for the ground state. We use the following notations; 'π_u' and 'π_g' denote the π-type bonding and antibonding orbitals localized on oxygen. The superscripts 'o' and 'p' as in 'π_u^o' and 'π_g^p' denote that the orbitals are on and perpendicular to the mirror plane, respectively. In Table 3, the orbital energies and characters are shown. The so-called 'four orbitals', $26a'$, $21a''$, $23a''$, and $27a'$ of the porphyrin ring are located around the HOMO–LUMO region, but the LUMO of oxyheme is the antibonding MO between the Fe d_{yz} and O_2 π_g^p orbitals and in $23a''$ MO (next LUMO), the oxygen π_g^p orbital mixes. The interaction between Fe and O_2 is classified into σ and π types. $17a'$ MO is localized on O_2 but has the nature of the σ donation from O_2 π_g^o to Fe d_z^2. $3a''$, $14a''$, and $22a''$ MOs represent Fe–O_2 π interaction which have 3-center 4-electron bond character, however $14a''$ MO is delocalized over the entire molecule and the $22a''$ MO (LUMO) is localized on the O_2 π_g^p orbital. The LUMO energy level is low, which is characteristic to oxyheme and affects its excited states, as shown below.

Table 2
Dimensions of the SAC/SAC-CI calculations for the singlet and triplet states oxyheme

State	Singlet state			Triplet state		
	before selection	N [a]	after selection	before selection	N [a]	after selection
oxy form						
SAC(ground state)						
A'	6567495	1	14799			
SAC-CI(excited states)						
A'	6567495	11	103107	9743589	3	41924
A''	6562755	11	112160	9744303	3	42928
deoxy form						
SAC(ground state)						
A'	6568552	1	13649			
SAC-CI(excited states)						
A'	6568552	3	50683	9744796	3	50068
A''	6561728	3	49357	9743096	3	55044

[a] N denotes the number of the reference states in the configuration selection procedure.

Table 3
Orbital energies and characters of some HF orbitals of oxyheme

Orbital	Orbital energy (eV)	Nature [a]
occupied orbitals		
$2a''$	-18.456	$O_2 \pi_u^p + por \, \sigma$
$3a''$	-18.073	$O_2 \pi_u^p + Fe \, d_{yz}$
:		
$15a'$	-14.079	$O_2 \pi_g^o + por \, \pi$
:		
$17a'$	-13.499	$O_2 \pi_g^o + Fe \, d_{z^2}$
$18a'$	-13.286	$O_2 \, \pi_g^o + Fe \, d_{xz}$
$13a''$	-12.720	$Fe \, d_{xz} + O_2 \, \pi_g^o + Fe \, p_z + Im \, \sigma + Fe \, s + por \, \sigma$
$19a'$	-12.405	$Fe \, d_{xz}$
:		
$14a''$	-12.157	$O(2)^{\, b} \, p_y - Fe \, d_{yz} + por \, \sigma + Fe \, p_y$
:		
$16a''$	-11.813	$Fe \, d_{xy}$
$17a''$	-11.555	$Fe \, d_{yz} - Im \, \pi$
:		
$23a'$	-9.418	$por \, \pi$
:		
$25a'$	-8.825	$Fe \, d_{xz} - por \, \pi$
$20a''$	-8.754	$Fe \, d_{yz} - por \, \pi$
$26a'$	-6.544	$por \, \pi$ (n-HOMO; 4-orbitals)
$21a''$	-6.035	$por \, \pi$ (HOMO; 4-orbitals)
unoccupied orbitals		
$22a''$	0.139	$O_2 \, \pi_g^p - Fe \, d_{yz}$ (LUMO)
$23a''$	0.420	$por \, \pi - O_2 \, \pi_g^p$ (n-LUMO; 4-orbitals)
$27a'$	0.428	$por \, \pi$ (4-orbitals)
:		
$38a'$	9.914	$Fe \, d_{z^2} - por \, \sigma$
$39a'$	10.062	$Fe \, d_{x^2-y^2} - por \, \sigma$
:		
$42a'$	10.740	$Fe \, d_{x^2-y^2} - por \, \sigma$
$43a'$	10.798	$Fe \, d_{z^2} - Fe \, p_x - por \, \sigma - Im \, \sigma - O(1)^{\, b} \, p_x$
:		
$46a'$	11.420	$Fe \, d_{z^2} - O_2 \, \pi_g^o - Im \, \sigma - por \, \sigma$
$47a'$	12.035	$Fe \, d_{x^2-y^2} - por \, \sigma$

[a] The plus (+) and minus (−) signs denotes the bonding and antibonding interaction, respectively.
[b] O(1) and O(2) atoms are illustrated in Fig. 1.

In Table 4, the ground state and some low-lying singlet and triplet states of oxyheme calculated by the SAC/SAC-CI method are summarized. In previous SCF [29] and SCF-CI [12] studies, some open-shell singlet and triplet states were calculated to be more stable than the closed-shell state. In CASSCF calculations [10], the closed-shell state was the ground state and the open-shell singlet state was by 0.7 eV above the ground state. In our SECI calculation, the open-shell triplet and singlet states ($O_2 \pi_g^o \rightarrow O_2 \pi_g^p$–Fe d_{yz}) lie, respectively, 0.86 eV below and 0.33 eV above the closed-shell state. The energy ordering is much changed by the SAC/SAC-CI treatment: the closed-shell state is the ground state and the open-shell triplet and singlet states lie by 0.47 and 1.54 eV above the ground state, respectively, as seen in Table 4. This result is consistent with the antiferromagnetic nature of oxyheme.

In the ground state, the configuration mixing lowers the state energy quite effectively, indicating a crucial role of electron correlation. The main configuration is the HF configuration, which mixes with several double excitations, e.g. from Fe–O_2 bonding to antibonding MOs.

The electronic structure of the Fe–O_2 bond in oxyheme is characterized by

$$Fe(II)(S = 0) + O_2(^1\Delta_g)(S = 0),\qquad (1)$$
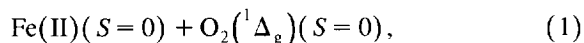
based on the electron population analysis and from the nature of the HF MOs. In Table 5, the Mulliken population analysis is given for the lowest five states shown in Table 4. In the ground state, the electron population of the Fe atom is roughly $(d_{xy})^2(d_{xz})^2-(d_{yz})^2$, and that for the the O_2 ligand is $(\pi_u^o)^2(\pi_u^p)^2-(\pi_g^o)^2$. In this point, our present result is different from Goddard's in which the population is $(d_{xy})^2-(d_{xz})^2(d_{yz})^1(d_{z^2})^1(\pi_u^o)^2(\pi_u^p)^2(\pi_g^o)^1(\pi_g^p)^1$ from their GVB-CI calculation [8]. A reason is that they used a seriously approximate model which ignored the porphin ring itself and imidazole. The net charge of the Fe atom in the ground state is almost +2 and that of the O_2 molecule is almost neutral, negating the superoxide structure of O_2 in the Weiss model. This result supports the Pauling model as most appropriate for the ground state of oxyheme among the models proposed, though the amount of the π back donation from Fe d_{yz} to O_2 π_g^p is small as shown in Table 5.

Harcourt [30] indicated that the electronic structure (1) based on the MO calculation may include the VB component corresponding to the Goddard model [7,8]. We examined therefore the present re-

Table 4
Ground and excited states of oxyheme in the two different geometries

State	Oxy form SAC/SAC-CI				exp.		Deoxy form SAC/SAC-CI
	excitation energy (eV)	main configuration	nature	oscillator strength (direction)	excitation energy (eV)	oscillator strength [a]	excitation energy (eV)
ground state							
X $^1A'$	0.0	$1.00(HF) - 0.15(3a'' \rightarrow 22a', 3a' \rightarrow 22a'')$ $+ 0.11(3a'' \rightarrow 22a'', 2a' \rightarrow 22a')$					0.0 [c]
excited state							
$1\,^3A''$	0.47	$0.66(17a' \rightarrow 22a') + 0.42(18a' \rightarrow 22a'')$ $-0.37(15a' \rightarrow 22a'')$	$O_2(\pi_g^o) \rightarrow O_2(\pi_g^p)$				-0.15 [d]
$1\,^1A''$	1.54	$0.63(17a' \rightarrow 22a') + 0.40(18a' \rightarrow 22a'')$ $-0.34(15a' \rightarrow 22a'')$	$O_2(\pi_g^o) \rightarrow O_2(\pi_g^p)$	$8.2 \times 10^{-5}\,(y)$	1.29 [a], 1.34 [b]	2.6×10^{-3}	0.67
$2\,^3A'$	1.95	$0.33(17a'' \rightarrow 38a') - 0.31(13a'' \rightarrow 38a')$	$Fe(d_{yz}) \rightarrow Fe(d_{z^2})$				1.55
$1\,^3A'$	1.97	$0.53(19a' \rightarrow 43a') + 0.52(19a' \rightarrow 38a')$	$Fe(d_{xz}) \rightarrow Fe(d_{z^2})$				
$2\,^1A'(Q_x)$	2.38	$0.65(21a' \rightarrow 23a') + 0.63(26a' \rightarrow 27a')$ $-0.32(21a' \rightarrow 22a')$	$por(\pi) \rightarrow por(\pi)$	$0.017\,(x, z)$	2.22 [a]	$0.12(Q_0)$	
$2\,^1A''$	2.44	$-0.62(26a \rightarrow 22a') - 0.55(21a'' \rightarrow 27a')$ $+ 0.47(26a' \rightarrow 23a'')$	$por(\pi) \rightarrow$ $O_2(\pi_g^p), por(\pi)$	$2.9 \times 10^{-4}\,(y)$			
$3\,^1A''(Q_y)$	2.64	$0.69(26a' \rightarrow 22a') + 0.50(26a' \rightarrow 23a'')$ $-0.39(21a' \rightarrow 27a')$	$por(\pi) \rightarrow$ $O_2(\pi_g^p), por(\pi)$	$0.0073\,(y)$			
$3\,^1A'$	2.71	$0.88(21a'' \rightarrow 22a') + 0.34(21a'' \rightarrow 23a'')$	$por(\pi) \rightarrow O_2(\pi_g^p)$	$8.7 \times 10^{-5}\,(x, z)$			
$4\,^1A''$	2.75	$-0.59(25a' \rightarrow 22a'') - 0.58(19a' \rightarrow 22a'')$	$Fe(d_{xz}) \rightarrow O_2(\pi_g^p)$	$3.0 \times 10^{-5}\,(y)$			
$5\,^1A''$	2.82	$-0.31(17a'' \rightarrow 38a')$	$Fe(d_{yz}) \rightarrow Fe(d_{z^2})$	$9.0 \times 10^{-5}\,(y)$			
$4\,^1A'$	2.83	$0.51(19a' \rightarrow 43a') + 0.48(19a' \rightarrow 38a')$ $+ 0.31(19a' \rightarrow 46a')$	$Fe(d_{xz}) \rightarrow Fe(d_{z^2})$	$0.0015\,(x, z)$			
$5\,^1A'$	3.02	$-0.68(20a' \rightarrow 22a') + 0.32(17a'' \rightarrow 22a'')$	$Fe(d_{yz}) \rightarrow O_2(\pi_g^p)$	$0.022\,(x, z)$			
$6\,^1A'$	3.08	$0.88(16a'' \rightarrow 22a'')$	$Fe(d_{xy}) \rightarrow O_2(\pi_g^p)$	$0.0010\,(x, z)$			
$6\,^1A''$	3.13	$-0.56(16a' \rightarrow 42a') + 0.51(16a'' \rightarrow 39a')$ $-0.40(16a' \rightarrow 47a')$	$Fe(d_{x^2-y^2}) \rightarrow Fe(d_{x^2-y^2})$	$5.0 \times 10^{-7}\,(y)$			

[a] Solution spectrum for horse oxyhemoglobin [33].
[b] Solution spectrum for horse oxyhemoglobin [32].
[c] The lowest singlet state of the deoxy form is higher by 4.11 eV than the ground state of the oxy form.
[d] Calculated lowest state of the deoxy form.

Table 5
Mulliken population analysis for the ground and excited states of oxyheme

	X ^{1}A′(SAC)	1 ^{3}A″	1 ^{1}A″	2 ^{3}A″	1 ^{3}A′
Fe (net charge)	1.9069	1.9068	1.9144	1.9601	1.9629
d_{x^2}	0.2061	0.1970	0.1998	0.2399	0.4699
d_{y^2}	0.2118	0.2019	0.2050	0.4658	0.2454
d_{z^2}	0.1576	0.1370	0.1400	0.7510	0.7497
d_{xy}	1.9837	1.9878	1.9876	1.9911	1.9912
d_{xz}	1.9761	1.9772	1.9654	1.9813	1.0344
O1 [a] (net charge)	0.0506	0.0158	0.0161	0.0326	0.0416
p_x	1.2443	1.1425	1.1449	1.2465	1.2420
p_y	1.0818	1.5167	1.5051	1.0815	1.0744
O2 [a] (net charge)	− 0.0134	0.0233	− 0.0053	0.0095	− 0.0070
p_x	1.2479	1.1319	1.1310	1.2489	1.2440
p_y	0.9884	1.5102	1.5221	0.9617	0.9850
p_z	1.8376	1.3951	1.4128	1.8401	1.8382
Por [b] (net charge)	− 1.7698	− 1.7728	− 1.7521	− 1.7982	− 1.7933
Im [c] (net charge)	− 0.1742	− 0.1731	− 0.1731	− 0.2038	− 0.2042

[a] The numbering of atoms are given in Fig. 1.

[b] Porphyrin ring.

[c] Imidazole.

sult using the Harcourt method and found that the component corresponding to the Goddard model little contributes to the present ground state of oxyheme. This is supported by a large difference in the electron distribution between the present result and the Goddard one [8].

4. Low-lying excited states

The nature of some low-lying singlet and triplet excited states are shown in Tables 4 and 5. The ordering is 1 ^{3}A″, 1 ^{1}A″, 2 ^{3}A″, and 1 ^{3}A′ which lie by 0.47, 1.54, 1.95, and 1.97 eV, respectively, above the ground state. The electronic structures of these states are represented as

$$1\,^3\text{A}'': \quad \text{Fe(II)}(S=0) + \text{O}_2\left(^3\Sigma_g^-\right)(S=1), \quad (2)$$

$$1\,^1\text{A}'': \quad \text{Fe(II)}(S=0) + \text{O}_2\left(^1\Sigma_g^+\right)(S=0), \quad (3)$$

$$2\,^3\text{A}'', 1\,^3\text{A}': \quad \text{Fe(II)}(S=1) + \text{O}_2\left(^1\Delta_g\right)(S=0). \quad (4)$$

Note that the energy ordering of the free O_2 molecule is $^3\Sigma_g^-$ (0.0 eV) $< ^1\Delta_g$ (0.98 eV) $< ^1\Sigma_g^+$ (1.64 eV) [31]. The 1 ^{1}A″ and 1 ^{3}A″ states arise by one electron excitation from the O_2 π_g^o MO to the O_2 π_g^p–d_{yz} MO (LUMO) and the 2 ^{3}A″ (1 ^{3}A′) state from Fe d_{yz} (d_{xz}) to d_{z^2}. Table 5 clearly shows the changes in the electron population by these transitions.

The excitations, X ^{1}A′ → 1 ^{3}A″ and X ^{1}A′ → 1 ^{1}A″, correspond to the reorganizations of the electronic structure of oxygen, namely, $^1\Delta_g$ → $^3\Sigma_g^-$ and $^1\Delta_g$ → $^1\Sigma_g^+$, respectively. We note that the 1 ^{3}A″ state has a very small excitation energy of 0.47 eV, since the LUMO energy level is very low and since the excitation is actually the relaxation of the O_2 electronic structure to its ground state, i.e. $^3\Sigma_g^-$. Therefore, the 1 ^{3}A″ state should be stabilized to a larger extent than the closed shell state as the Fe–O_2 distance is separated. These results suggest that the 1 ^{3}A″ state has a possibility to participate in the O_2 capture and release process of heme.

In Fig. 2, the absorption spectrum of oxyhemoglobin [32] and the SAC-CI theoretical spectrum are compared in the region of below 3 eV. The calculated spectrum well reproduces the experimen-
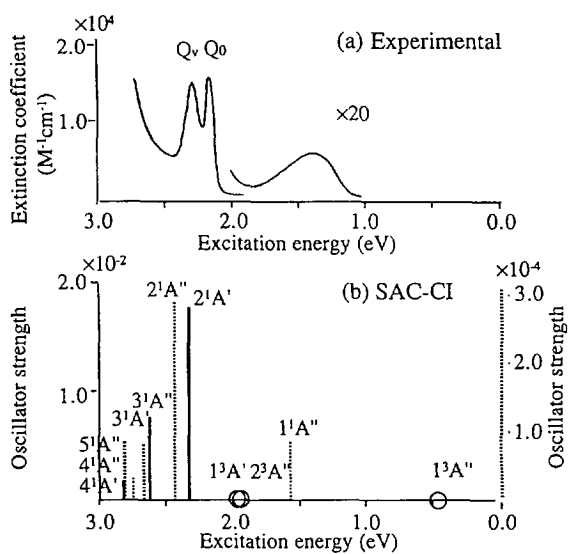
Fig. 2. Electronic spectrum of oxyheme. (a) Experimental spectrum of horsehemoglobin [32]. (b) SAC-CI theoretical spectrum. Open circles denote triplet excited states. Left and right vertical axes correspond to the spectral intensities drawn by the real and dotted lines, respectively.

tal one. The first peak at about 1.34 eV is assigned to the $1\,^1A''$ state which is characterized as the $^1\Delta_g \rightarrow{}^1\Sigma_g^+$ excitation within O_2 ligand, as described above. This assignment is confirmed by comparing the absorption spectrum of the horse oxyhemoglobin with that of the carboxyhemoglobin [32]: the peak at 1.34 eV exists in the former but not in the latter. The second and third absorptions, called the Q band, are assigned to the $2\,^1A'$ and $3\,^1A''$ states, respectively. These Q bands look similar to those of FBP, but a difference is that the five orbitals, instead of the four orbitals, are involved in the excitations. In addition to the so-called four orbitals, the LUMO which is localized in the $Fe-O_2$ region also participates in the Q bands as seen from Table 4.

At the energies 2.82, 2.83, and 3.13 eV, there exist 3 excited states originating from the Fe d-orbitals, which are roughly characterized as the ligand field d–d excitations within the Fe atom. The intensities are therefore quite small. The excitations calculated at 2.75, 3.02, and 3.08 eV are the electron transfer transitions from Fe d-orbital to oxygen. These excited states have the electronic structure represented by the Weiss model [9].

In a previous study [33], some very weak peaks were observed at the lower energy side of the 1.34 eV peak. We may qualitatively assign these peaks to the triplet states, however, more decisive assignment is difficult at the present stage of the calculation.

5. Ground and excited states in the deoxy form

Next we calculate the low-lying singlet and triplet states of oxyheme in a deformed geometry, i.e. in the 'deoxy form'. The aim is to examine the effect of the deformation on the relative stability of the low-lying singlet and triplet states. An X-ray crystal structure analysis [22] showed that in deoxyheme the porphyrin ring moves towards the sixth sites by 0.6 Å along the $Fe-N_{Im}$ axis. The results of the SAC-CI calculation for this geometry are shown in Table 4.

In the deoxy form, the closed-shell state become unstable, lying over the triplet $1\,^3A''$ state by 0.15 eV. This indicates that if some geometrical change is induced to oxyheme through a conformational change of the heme protein, the O_2 affinity of heme is lowered, facilitating the $Fe-O_2$ bond breaking process. Though the $1\,^3A''$ state in the present deoxy form is 3.95 eV (90 kcal/mol) higher than the X $^1A'$ state of the oxy form, the activation energy should be much smaller than this value, since we did not consider any geometric relaxation effect in this calculation. The X $^1A' \rightarrow 1\,^3A''$ transition would occur at the geometry between the oxy and the deoxy form. More detailed study on this process is in progress.

Acknowledgements

References

[1] W.D. Scheidt and C.A. Reed, Chem. Rev. 81 (1981) 543; Y. Nishida, Inorganic biological chemistry (Shokado, Tokyo, 1994) pp. 26–58.

[2] L. Pauling and C.D. Coryell, Proc. Natl. Acad. Sci. US 22 (1936) 210.

[3] M. Montenteau and C.A. Reed, Chem. Rev. 94 (1994) 659.

[4] I. Bytheway and M.B. Hall, Chem. Rev. 94 (1994) 639.

[5] J.P. Collman, R.R. Gage, C.A. Reed, W.T. Robinson and G.A. Rodley, Proc. Natl. Acad. Sci. US 71 (1974) 1326.

[6] L. Pauling, Stanford Med. Bull. 6 (1948) 215; Nature 203 (1964) 182.

[7] D.S. Maclure, Radiation Res. Suppl. 1 (1960) 218; R.D. Harcount, Lecture note in chemistry, Vol 30. Qualitative valence bond descriptions of electron-rich molecules (Springer, Berlin, 1982) p. 205; B.D. Olafson and W.A. Goddard III, Proc. Natl. Acad. Sci. US 74 (1977) 1315.

[8] W.A. Goddard III and B.D. Olafson, Proc. Natl. Acad. Sci. US 72 (1975) 2335.

[9] J.J. Weiss, Nature 202 (1964) 83.

[10] S. Yamamoto and H. Kashiwagi, Chem. Phys. Letters 161 (1989) 85; 206 (1993) 306.

[11] J.E. Newton and M.B. Hall, Inorg. Chem. 23 (1984) 4627.

[12] M.-M. Rohmer, Mathematical and physical sciences, Vol. 176 (Reidel, Dordrecht, 1986) p. 377.

[13] H. Nakatsuji and K. Hirao, J. Chem. Phys. 68 (1978) 2035.

[14] H. Nakatsuji, Chem. Phys. Letters 59 (1978) 362; 67 (1979) 329, 334.

[15] H. Nakatsuji, Acta Chim. Hung. 129 (1992) 719.

[16] H. Nakatsuji, J. Hasegawa and M. Hada, J. Chem. Phys., in press.

[17] J. Geertsen, M. Ritby and R.J. Bartlett, Chem. Phys. Letters 164 (1989) 57; S.R. Gwaltney and R.J. Bartlett, Chem. Phys. Letters 241 (1995) 26.

[18] H. Nakatsuji and M. Ehara, J. Chem. Phys. 101 (1994) 7658.

[19] S.E.V. Phillips, J. Mol. Biol. 142 (1980) 531; Nature 273 (1978) 247.

[20] H. Sekino and H. Kobayashi, J. Chem. Phys. 86 (1987) 5045.

[21] J.E.D. Bene and I. Cohen, J. Am. Chem. Soc. 100 (1978) 5285.

[22] G. Fermi, J. Mol. Biol. 97 (1975) 237.

[23] S. Huzinaga, J. Andzelm, M. Klobukowski, E. Radzio-Andzelm, E. Sakai and H. Tatewaki, Gaussian basis set for molecular calculations (Elsevier, Amsterdam, 1984).

[24] S. Huzinaga, J. Chem. Phys. 42 (1965) 1293.

[25] H. Nakatsuji, Chem. Phys. 75 (1983) 425.

[26] M. Dupuis and A. Farazdel, MOTECC-91 (Center for Scientific and Engineering Computations, IBM Corporation, 1991).

[27] H. Nakatsuji, M. Hada, H. Nakai and J. Hasegawa, the accelerated version of SAC85, to be published.

[28] H. Nakatsuji, Program System for SAC and SAC-CI Calculations (Program Library No.146 (Y4/SAC), Data Processing Center of Kyoto University, 1985); Program Library SAC85 No. 1396, (Computer Center of the Institute for Molecular Science, 1981).

[29] T. Nozawa, M. Hatano, U. Nagashima, S. Obara and H. Kashiwagi, Bull. Chem. Soc. Japan 56 (1983) 1721.

[30] R.D. Harcourt, Chem. Phys. Letters 167 (1990) 374.

[31] K.P. Huber and G. Herzberg, Molecular spectra and molecular structure, Vol. 3 (Van Nostrand Reinhold, New York, 1979).

[32] M.W. Makinen and W.A. Eaton, Ann. NY Acad. Sci. 206 (1973) 210.

[33] W.A. Eaton, L.K. Hanson, P.J. Stephans, J.C. Sutherland and J.B.R. Dunn, J. Am. Chem. Soc. 100 (1978) 4991.